Catalysis Letters Vol. 108, Nos. 1–2, April 2006 (© 2006)
DOI: 10.1007/s10562-006-0029-7

Removal of nitric oxide over Saskatchewan lignite and its derivatives

Goutam Chattopadhyaya, Douglas G. Macdonald, Narendra N. Bakhshi, Jafar S. Soltan Mohammadzadeh, and Ajay K. Dalai*

Catalysis and Chemical Reaction Engineering Laboratories, Department of Chemical Engineering, University of Saskatchewan, 57 Campus Drive, Saskatoon, SK S7N 5A9, Canada

Received 20 September 2005; accepted 24 January 2006

Adsorption of nitric oxide was studied over reduced and unreduced Fe, Cu, Co and Ni impregnated activated carbons (AC) in a microreactor system in the presence and absence of oxygen. In the absence of oxygen reduced Fe–AC showed an NO removal efficiency of 58% which was higher than that of virgin activated carbon by a factor of 2.5. The removal efficiency of Cu–AC with and without oxygen was in the range of 44–46%.

KEY WORDS: activated carbon; nitric oxide adsorption; Saskatchewan lignite.

1. Introduction

NO_x emissions have been linked to the urban smog, acid rain and formation of ozone. Fossil-fuel fired power plants are the major source of NO_x pollution in atmosphere. Due to stringent environmental regulations, intensive efforts are being made towards removal of NO_x from power plant flue gases.

Selective Catalytic Reduction (SCR) process [1] is considered to be one of the best available commercial technologies for removal of NO_x from stationary sources such as power plants. In this process, NO_x is selectively reduced to nitrogen in the presence of oxygen over supported vanadia catalyst using ammonia as the reductant at temperatures ranging from 350 to 450 °C [2–4]. Because of the good activity of the SCR catalyst at the high operating temperature the location of the SCR unit is restricted in the power plant. Therefore, what is needed is a process or a catalyst which can work at low operating temperatures; otherwise, extensive flue gas reheating will be required.

Activated carbon has been used as a catalyst for SCR of NO_x using ammonia at relatively lower temperatures ranging from 90 to 190 °C [5,6] while it has been indicated that impregnation of activated carbon with various metals including copper improves the activity of activated carbon further [7–10]. Though considerable research has been carried out on the SCR of NO_x on various activated carbons, very little information is available on the adsorption characteristics of NO_x on lignite, lignite-derived char and activated carbon, and metal-impregnated activated carbon. Application of low-cost lignite-derived adsorbents can have favorable effect on economic indicators of the process.

In this work, the NO_x adsorption characteristics of a Saskatchewan lignite, lignite-derived char and activated carbon, and metal-oxide impregnated activated carbon were studied in order to determine the potential of lignite for SCR processes and to provide an understanding of the reactive adsorption process resulting in NO_x removal. A thorough physical characterization of all the adsorbents were carried out and the effect of oxygen on the NO_x adsorption was investigated.

2. Experimental

Char was prepared by the carbonization of dried lignite at a carbonization temperature of 475 °C and holding time of 120 min in flowing nitrogen. The resulting char was subsequently activated with steam at 650 °C for 15 min and then dried overnight at 110 °C. Details on the preparation and characterization of lignite, lignite-derived char and activated carbon were reported previously [11]. These operating conditions resulted in producing the adsorbents with most desirable properties and highest micropore surface area and pore volume.

Metal-impregnated activated carbons were prepared by incipient wetness impregnation technique using aqueous solutions of copper, iron, cobalt and nickel nitrate analytical grade salts (BDH Chemicals). The 1% (wt) metal loaded activated carbons were dried at 110 °C for 24 h. The low metal loading in this work ensured minimum reduction in surface area and pore volume of the activated carbon support [7].

Micropore surface area, micropore volume, micropore size and size distribution of the activated carbon as

---

* To whom correspondence should be addressed.
E-mail: ajay.dalai@usask.ca

well as metal-impregnated activated carbons were determined in an accelerated surface area and porosimetry instrument (ASAP 2000, Micromeritics) using CO_2 as the analysis gas at an analysis temperature of 0 °C. Prior to the analysis, each sample was degassed at 125 °C for 24 h. Micropore surface area was calculated using Dubinin–Astakhov equation [12]. Micropore volume and pore size distribution were estimated by Horvath–Kawazoe method [13].

Lignite, char, activated carbon and various metal-impregnated activated carbon adsorbents were subjected to NO adsorption experiments in the presence and absence of oxygen.

Figure 1 shows the process flow diagram of the experimental set-up used for the NO adsorption studies. The adsorber consisted of a stainless steel (SS-326) tubular reactor (12.7 mm ID and 450 mm overall length) placed in an electrically heated furnace. The furnace temperature was controlled by a series SR22 microporcessor-based auto-tuning PID controller (Shimaden Co., Tokyo, Japan) through a K-type thermocouple inserted into a heating block placed concentrically within the furnace. A separate thermocouple was used to monitor the reactor bed temperature. A multichannel digital temperature indicator was used to record the temperatures (Shimaden Co., Tokyo, Japan).

Needle valves were used to control the flow rates of N_2, NO and O_2. While the flow rate of N_2 was monitored by a type 8141 Matheson transducer connected to a mass flow meter readout model 8143, flow rates of NO and O_2 were monitored by two pre-calibrated rotameters.

Gases were analyzed for NO using on-line Hewlett-Packard 5890A gas chromatograph with a thermal conductivity detector (TCD) and a 1.82 m long stainless steel column containing 60/80 Chromosorb-102 maintained at 90 °C.

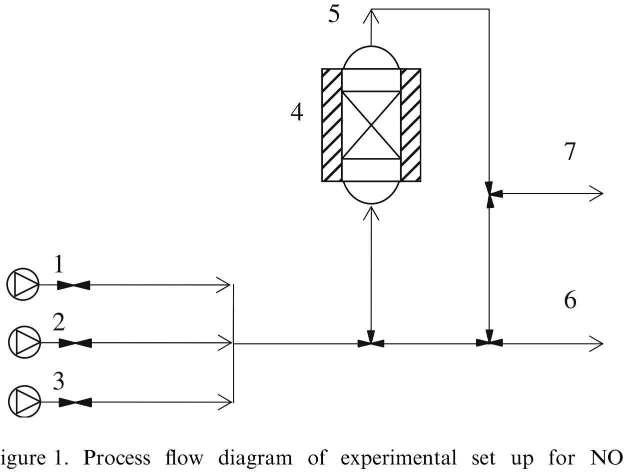

Figure 1. Process flow diagram of experimental set up for NO adsorption on lignite, char, and activated carbons (1-N_2, 2-NO, 3-O_2, 4-heater, 5-reactor, 6-gas to analyzer, and 7-gas to vent).

Operating parameters for the nitric oxide adsorption experiments in the presence and absence of O_2 were as follows: particle size, 4 mm; adsorption temperature, 125 °C; residence time, 4 s; feed NO concentration, 400–1100 ppm; and feed O_2 concentration 0 and 6.5%. For a typical adsorption run the reactor was packed with a mixture of 1 g of the adsorbent and 3 g of glass beads (both in the same particle size range). Prior to the NO adsorption experiments, all the metal-impregnated activated carbon adsorbents were heated *in situ* at 375 °C in flowing nitrogen. Some NO adsorption experiments were performed using impregnated adsorbents which were reduced *in situ* at 375 °C in a H_2 atmosphere (60–75 mL/min) for 2 h. After these pretreatments, the reactor was cooled to the desired adsorption temperature in flowing 99.995% pure nitrogen (Linde, Edmonton, Canada) and was held at that temperature for 1 h. Then the pure nitrogen gas flow was stopped and the NO gas mixture containing the desired concentration of NO and O_2 was passed through the adsorbent bed at the desired flow rate. The effluent stream was analyzed at 5 min intervals to determine the effluent NO concentration. Appropriate repeat and calibration runs ensured reliable analysis results.

3. Results and discussions

NO adsorption characteristics of lignite and lignite-derived char, activated carbon and metal-impregnated activated carbons, were evaluated by generating experimental breakthrough curves (a plot of the ratio of outlet/inlet concentrations during the run). The overall NO removal efficiency was calculated from the information concerning the total amount of NO that was fed into the reactor (NO_{in}) and total amount of NO that left the reactor un-adsorbed (NO_{out}) during the adsorption experiment.

3.1. NO adsorption on lignite, char and activated carbon

Figure 2 shows the NO breakthrough profiles on lignite, lignite-derived char and activated carbon while table 1 gives the comparison of the NO removal efficiency on various adsorbents in the presence and absence of oxygen. Table 2 shows the physical characteristics of lignite-derived adsorbents.

It can be seen from figure 2 that there is no significant difference in the breakthrough times for NO on lignite (surface area of 27 m^2/g), char (surface area of 136 m^2/g) and lignite-derived activated carbon (surface area of 185 m^2/g). However, in the case of lignite, once NO broke through the bed, the effluent NO concentration reached the influent NO concentration rapidly and thus adsorption of nitric oxide on lignite was negligible after the breakthrough point. In contrast, in the case of char and activated carbon, it was observed that no complete breakthrough of NO was achieved; that is, the effluent

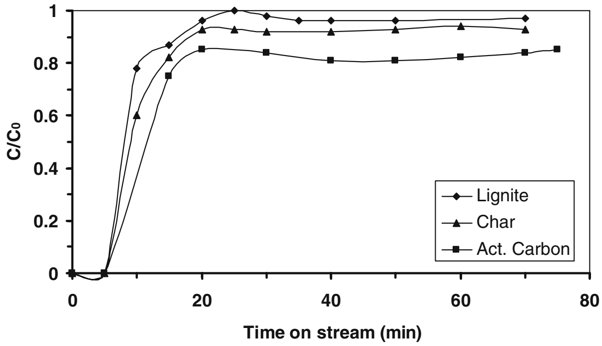

Figure 2. Comparison of breakthrough curves of NO on lignite, char, and activated carbon (Feed NO concentration, 1100 ppm; Residence time, 4s; Adsorption temperature, 125°C).

NO concentration remained less than the influent NO concentration over the time period studied. Thus, an appreciable amount of NO has been removed by car and activated carbon after the breakthrough point. This is reflected in the higher removal efficiency of char and activated carbon as given in table 1. For example, the overall NO removal efficiency of activated carbon (22.7%) is significantly higher than that of the lignite (7.9%). The higher removal of NO on char and activated carbon can be attributed to the higher micropore surface area of the lignite-derived adsorbents.

3.2. *NO oxide adsorption on metal-impregnated activated carbons*

The effects of metal impregnation on activated carbons on NO removal are shown in table 1 in the form of removal efficiencies and breakthrough times. It can be seen that impregnation of activated carbon with iron additives improved the breakthrough time and consequently the NO removal efficiency. However there was marginal increase in the overall NO removal efficiency of Fe/AC (24.5%) in comparison to activated carbon alone (22.7%). This phenomenon can be explained using the results obtained from the physical characterization of the adsorbents which is shown in table 2. The micropore volume and micropore surface area did not change significantly due to addition of iron to activated carbon (before calcinations). So, impregnation of the activated carbon with ferric nitrate resulted in the distribution of the active species mostly on the outer surface of the activated carbon granule. However, calcination of Fe/AC adsorbent (heating at 375 °C in nitrogen) resulted in a significant decrease in both the micropore volume and surface area indicating that the migration of iron oxide into the porous system may have taken place. However, the increase in the overall NO removal efficiency due to addition of iron could not compensate for the decrease in adsorption due to the loss in microporosity, resulting in a net decrease in the

Table 1
Comparison of the NO removal efficiency (R.E.) and breakthrough time (t_b) for various lignite-derived adsorbents for a feed gas containing 1100 ppm NO

Adsorbent	In the absence of oxygen				In the presence of oxygen			
	NO_{in} (g)	NO_{ads} (g)	R.E. (%)	t_b (min)	NO_{in} (g)	NO_{ads} (g)	R.E. (%)	t_b (min)
Lignite	14.0	1.1	7.9	5.1	–	–	–	–
Char	14.0	2.4	17.1	5.1	–	–	–	–
AC	15.0	3.4	22.7	5.3	–	–	–	–
AC[a]	2.7	0.7	25.9	7.1	8.0	2.9	36.2	11.5
Fe/AC	11.0	2.7	24.5	5.1	–	–	–	–
Fe/AC (R[b])	24.0	14.0	58.3	30.4	16.0	7.1	44.4	16.8
Cu/AC (R)	24.0	10.7	44.6	10.5	10.0	4.6	46.0	18.9
Co/AC (R)	–	–	–	–	4.0	1.8	45.0	–
Ni/AC (R)	–	–	–	–	8.0	3.8	47.5	18.0

[a] Influent NO concentration 400 ppm.
[b] Catalysts were reduced in hydrogen at 375 °C for 2h.

Table 2
Physical characteristics of lignite-derived adsorbents

Physical characteristic	Lignite	Char	AC	Fe/AC		Cu/AC		Co/AC		Ni/AC	
				Uncal.	Cal.	Uncal.	Cal.	Uncal.	Cal.	Uncal.	Cal.
Micropore volume, cc/g	0.014	0.082	0.085	0.084	0.065	0.064	0.068	0.054	0.067	0.057	0.072
Micropore surface area, m^2/g	27	136	185	170	110	130	145	117	144	117	149
Median pore diameter Å	9.3	6.8	8.3	8.5	12.6	8.8	7.7	8.5	7.6	8.7	8.6

overall NO removal efficiency. A similar observation was reported in the literature [14].

Expectedly the low influent NO concentrations result in long breakthrough times and consequently, a better adsorption performance. For example, the overall NO removal efficiency on activated carbon adsorbent with an influent NO concentration of 400 ppm was higher (25.9%) than that with 1100 ppm (22.7%).

Chemisorption of NO on the transition metal oxides is affected by the oxidation state of the metal species [9,15]. In figure 3 the NO breakthrough profiles on unreduced and reduced Fe/AC are presented. Figure 3 shows that there was a significant improvement in the breakthrough time due to *in situ* reduction of Fe/AC adsorbent by pure hydrogen compared to the unreduced Fe/AC adsorbent. The NO breakthrough time improved from 5.1 to 30.4 min. This resulted in a significant increase in the overall NO removal efficiency of the reduced Fe/AC adsorbent compared to that of the unreduced Fe/AC. Table 1 also shows that reduced Cu/AC adsorbent exhibited considerable improvement in the NO removal efficiency over activated carbon alone. The overall NO removal efficiency for activated carbon and reduced Cu/AC were 22.7% and 44.6%, respectively.

3.3. NO adsorption in the presence of oxygen

In any reaction involving the reduction of NO by a reducing agent, it is important to determine whether the use of the reducing agent is selective for nitric oxide as opposed to a reaction in which oxygen competes with NO for the same reducing agent. Therefore, the effect of oxygen on the NO removal over various lignite-derived adsorbents was studied using the reference operating conditions of: adsorption temperature of 125 °C, residence time of 4 s, influent NO concentration of 400 ppm and influent oxygen concentration of 6.5%. As reduced metal-impregnated activated carbon adsorbents were found to perform better than the unreduced ones, NO adsorption experiments, in the presence of oxygen, were carried out with reduced adsorbents (Fe/AC, Cu/AC, Co/AC and Ni/AC).

Table 1 shows a comparison between the overall NO removal efficiencies of the various adsorbents and the NO breakthrough times on activated carbon in the presence and absence of oxygen while figure 4 compares the NO breakthrough profiles.

It can be seen from figure 4 and table 1 that in the presence of oxygen, the breakthrough time for activated carbon increased from 7.1 min in the absence of oxygen to 11.5 min in the presence of oxygen. Also, it can be seen from table 1 that in the presence of oxygen, the overall NO removal efficiency of activated carbon increased from 25.9% to 36.2%. This was due to the higher activity of reactive adsorption of nitric oxide in the presence of oxygen. Similar observation was made by Richter [5].

Table 1 shows that except for reduced Fe/AC adsorbent, the presence of oxygen improved the overall NO removal efficiencies and breakthrough times of all the adsorbents. It is interesting to note that in the case of reduced Fe/AC adsorbent, the presence of oxygen reduced the NO removal efficiency from 58.3% to 44.4% while the NO breakthrough time decreased from 30.4 to 16.8 min. This phenomenon can be attributed to the partial reoxidation of iron by adsorbed NO or oxygen. However, the overall NO removal efficiency of the reduced Fe/AC in the presence of oxygen (44.4%) was still higher than the removal efficiency of the unreduced Fe/AC adsorbent in the absence of oxygen (24.5%).

The overall NO removal efficiency followed the order: Ni/AC > Cu/AC > Co/AC > Fe/AC however, the difference in their performances was not very pronounced. This behavior can be explained on the basis of the microporosity characteristics of the adsorbents as shown in table 2. Table 2 shows that the micropore

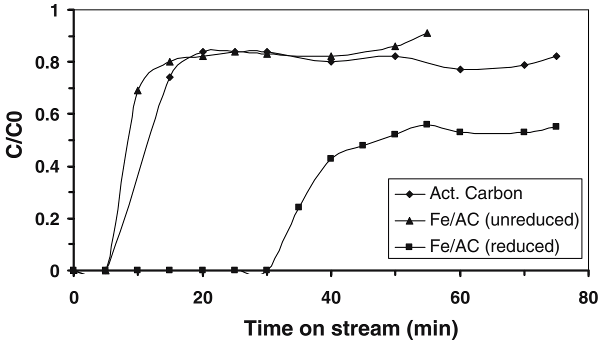

Figure 3. Comparison of breakthrough curves of NO on activated carbon (AC), reduced and unreduced Fe-impregnated activated carbon (Feed NO concentration, 1100 ppm; Residence time, 4s; Adsorption temperature, 125°C).

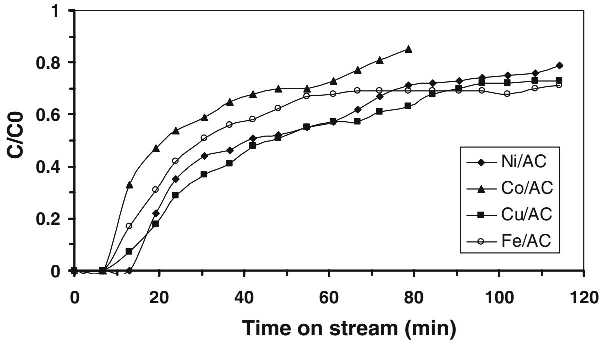

Figure 4. Breakthrough profiles of NO on reduced Fe-, Cu-, Co-, and Ni-impregnated activated carbon in the presence of oxygen (Feed concentration: NO, 400 ppm; O_2, 6.5% in N_2, Residence time, 4s; Adsorption temperature, 125°C).

volume and surface area of the calcined metal-impregnated activated carbon adsorbents decreased in the same order as their overall NO removal efficiency. However, in the case of calcined Fe/AC adsorbent the micropore surface area was significantly lower compared to the other impregnated adsorbents. Even though the literature [2] indicates no direct correlation of the BET surface area and pore volume of the adsorbents with their NO removal efficiency, these results show that the NO removal efficiency is related to micropore parameters such as micropore volume and microproe surface area. The NO removal efficiency of the adsorbents was observed to increase with increase in the the micropore volume and surface area of an adsorbent.

4. Conclusions

Adsorptive removal of NO using activated carbon and metal impregnated activated carbon was studied in both the absence and presence of O_2. In the absence of oxygen, lignite and lignite-derived char and activated carbon exhibited low NO removal efficiency. However, a significant improvement in the NO removal efficiency (58.3%) was achieved using the reduced Fe/AC adsorbent. In the presence of oxygen, the overall NO removal efficiency of reduced Cu/AC, Co/AC, and Ni/AC adsorbents increased while that of reduced Fe/AC decreased (compared to NO removal in absence of oxygen). The NO removal efficiency of adsorbents increased with increasing micropore volume and surface area.

Acknowledgments

Financial support from the Saskatchewan Power Corporation, and the University of Saskatchewan is gratefully acknowledged. JSSM gratefully acknowledges merit scholarship from Islamic Development Bank and research leave from Sahand University of Technology, Tabriz, Iran.

References

[1] Y.A. Li and J.N. Armor, US Pat., 5,149,512, 1992.
[2] S.A. Ahmed, J. Stencel, F. Derbyshire and B. Baldwin, Fuel 72 (1993) 287.
[3] Y. Wang, Z. Liu, L. Zhan, Z. Huang, Q. Liu and J. Ma, Chem. Eng. Sci. 59 (2004) 5283.
[4] Y. Wang, Z. Huang, Z. Liu and Q. Qingya Liu, Carbon 42 (2004) 445.
[5] E. Richter, Catal. Today 7 (1990) 93.
[6] L. Singoredjo, M. Slagt, J.V. Wees, F. Kapteijn and J.A. Moulijn, Catal. Today 7 (1990) 157.
[7] S. Park and J. Shin, J. Colloid Interface Sci. 264 (2004) 39.
[8] H. Tseng, M. Wey, Y.Y. Liang and K. Chen, Carbon 41 (2003) 1079.
[9] C. Marquez-Alvarez, I. Rodriguez-Ramos and A. Guerrero-Ruiz, Carbon 34 (1996) 1509.
[10] C. Marquez-Alvarez, I. Rodriguez-Ramos and A. Guerrero-Ruiz, Carbon 34 (1996) 339.
[11] G. Chattopadhyaya, D.G. Macdonald, N.N. Bakhshi, J.S. Soltan Mohammazadeh and A.K Dalai, Fuel, in press (2005).
[12] M.M. Dubinin, Carbon 27 (1989) 457.
[13] G. Horvath and K.J. Kawazoe, Chem. Eng. Jpn 16 (1983) 470.
[14] T. Grzybek, Appl. Catal. B: Environ. 1 (1992) 271.
[15] M. Shelef and J.T. Kumar, in: *Chemical Engineering Progress Symposium Series*, J.N. Butt and R.W. Coughlin eds, 115(67) (1971) 74.